

Molecular moieties masking Ca^{2+} -dependent facilitation of voltage-gated $\text{Ca}_v2.2$ Ca^{2+} channels

Jessica R. Thomas,^{1,2} Jussara Hagen,¹ Daniel Soh,⁵ and Amy Lee^{1,3,4}

¹Department of Molecular Physiology and Biophysics, ²Interdisciplinary Graduate Program in Neuroscience, ³Department of Otolaryngology Head-Neck Surgery, and ⁴Department of Neurology, University of Iowa, Iowa City, IA

⁵Medical Sciences Program, Boston University, Boston, MA

Voltage-gated $\text{Ca}_v2.1$ (P/Q-type) Ca^{2+} channels undergo Ca^{2+} -dependent inactivation (CDI) and facilitation (CDF), both of which contribute to short-term synaptic plasticity. Both CDI and CDF are mediated by calmodulin (CaM) binding to sites in the C-terminal domain of the $\text{Ca}_v2.1$ α_1 subunit, most notably to a consensus CaM-binding IQ-like (IQ) domain. Closely related $\text{Ca}_v2.2$ (N-type) channels display CDI but not CDF, despite overall conservation of the IQ and additional sites (pre-IQ, EF-hand-like [EF] domain, and CaM-binding domain) that regulate CDF of $\text{Ca}_v2.1$. Here we investigate the molecular determinants that prevent $\text{Ca}_v2.2$ channels from undergoing CDF. Although alternative splicing of C-terminal exons regulates CDF of $\text{Ca}_v2.1$, the splicing of analogous exons in $\text{Ca}_v2.2$ does not reveal CDF. Transfer of sequences encoding the $\text{Ca}_v2.1$ EF, pre-IQ, and IQ together (EF-pre-IQ-IQ), but not individually, are sufficient to support CDF in chimeric $\text{Ca}_v2.2$ channels; $\text{Ca}_v2.1$ chimeras containing the corresponding domains of $\text{Ca}_v2.2$, either alone or together, fail to undergo CDF. In contrast to the weak binding of CaM to just the pre-IQ and IQ of $\text{Ca}_v2.2$, CaM binds to the EF-pre-IQ-IQ of $\text{Ca}_v2.2$ as well as to the corresponding domains of $\text{Ca}_v2.1$. Therefore, the lack of CDF in $\text{Ca}_v2.2$ likely arises from an inability of its EF-pre-IQ-IQ to transduce the effects of CaM rather than weak binding to CaM per se. Our results reveal a functional divergence in the CDF regulatory domains of Ca_v2 channels, which may help to diversify the modes by which $\text{Ca}_v2.1$ and $\text{Ca}_v2.2$ can modify synaptic transmission.

INTRODUCTION

Voltage-gated Ca_v Ca^{2+} channels are multi-subunit complexes that regulate a variety of biological activities such as gene expression, muscle contraction, and neurotransmitter release. Ca_v channels consist of an α_1 subunit, which forms the pore, and two auxiliary subunits, β and $\alpha_2\delta$ (Simms and Zamponi, 2014). Of the multiple Ca_v channels that have been characterized ($\text{Ca}_v1.x$ – $\text{Ca}_v3.x$), $\text{Ca}_v2.1$ (P/Q-type) and $\text{Ca}_v2.2$ (N-type) channels play prominent presynaptic roles in regulating neurotransmitter release (Dunlap et al., 1995). $\text{Ca}_v2.1$ Ca^{2+} signals promote exocytosis at most synapses, including CA3-CA1 hippocampal synapses (Wheeler et al., 1994), the calyx of Held auditory brainstem synapse (Forsythe et al., 1998; Inchauspe et al., 2004), and the parallel fiber–Purkinje cell synapse in the cerebellum (Mintz et al., 1995). Although $\text{Ca}_v2.2$ plays a secondary role to $\text{Ca}_v2.1$ at many central synapses, $\text{Ca}_v2.2$ is the major Ca_v channel regulating neurotransmitter release from terminals of spinal nociceptive neurons (Hatakeyama et al., 2001) and superior cervical ganglion neurons (Boland et al., 1994). Genetic inactivation of $\text{Ca}_v2.2$ in mice causes no overt phenotypes except for higher pain thresholds (Hatakeyama et al., 2001). In contrast, knockout of $\text{Ca}_v2.1$ causes ataxia, seizures, and premature death (Jun et al., 1999).

Perhaps to support their distinct physiological roles, $\text{Ca}_v2.1$ and $\text{Ca}_v2.2$ channels are differentially modulated by a variety of factors, including the Ca^{2+} ions that pass through the pore. Like other high voltage-activated Ca_v channels (Liang et al., 2003), $\text{Ca}_v2.1$ and $\text{Ca}_v2.2$ undergo Ca^{2+} -dependent inactivation (CDI) mediated by calmodulin (CaM) binding to sites in the intracellular C-terminal domain (CTD) of the α_1 subunit (Lee et al., 1999; DeMaria et al., 2001). These include a consensus IQ-like domain for binding CaM (IQ) as well as a CaM-binding domain (CBD; Fig. 1). During a train of depolarizations, the amplitude of $\text{Ca}_v2.1$ Ca^{2+} currents increases and then declines because of the onset of CDI. The initial increase is caused by Ca^{2+} -dependent facilitation (CDF), which also requires CaM (Lee et al., 1999; DeMaria et al., 2001) and potentially other Ca^{2+} sensor proteins in neurons (Tsujimoto et al., 2002). CDF and CDI of $\text{Ca}_v2.1$ currents contribute to the facilitation and depression, respectively, of synaptic transmission at the calyx of Held (Cuttle et al., 1998; Forsythe et al., 1998; Tsujimoto et al., 2002) and other brain synapses (reviewed in Catterall et al., 2013).

Despite the physiological importance of CDF of $\text{Ca}_v2.1$ in short-term synaptic plasticity (Nanou et al., 2016),

Correspondence to Amy Lee: amy-lee@uiowa.edu



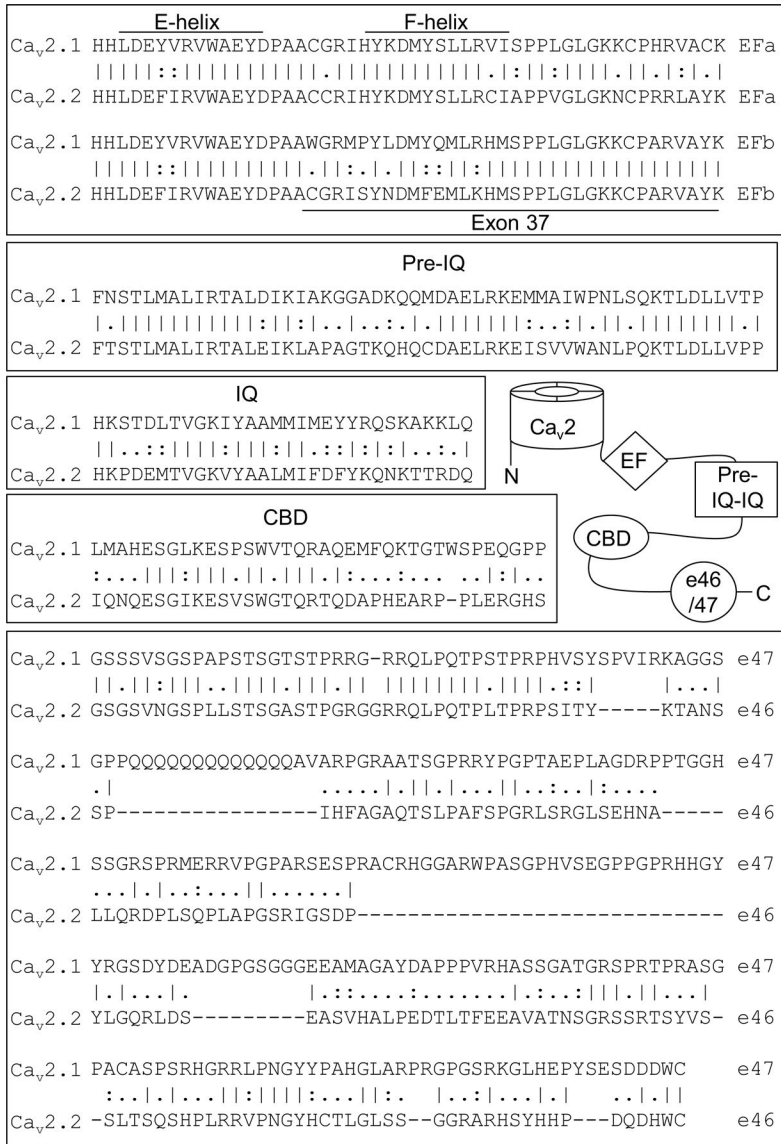


Figure 1. CDF modulatory domains in the CTD of Ca_v2.1 and sequence alignment with analogous regions of Ca_v2.2. Vertical bars (|), identical residues; colons (:), conservative substitutions; periods (.), nonconservative substitutions. Alignment is with human Ca_v2.1 and 2.2 sequences (GenBank NM_023035.2, NM_001127222.1, NM_000718.3, and CM000671.2).

there is little evidence that Ca_v2.2 channels are similarly regulated. In a heterologous expression system, CDF is not observed for Ca_v2.2 under conditions that evoke robust CDF of Ca_v2.1 (Liang et al., 2003). At the calyx of Held of mice lacking Ca_v2.1, Ca_v2.2 channels compensate for the loss of Ca_v2.1, but the resulting Ca²⁺ currents do not facilitate or support short-term plasticity (Inchauspe et al., 2004). Although a form of CDF has been reported for Ca_v2.2 channels in dorsal root ganglion neurons, the mechanism relies on CaM-dependent protein kinase II and is distinct from CaM-dependent CDF of Ca_v2.1 channels (Tang et al., 2012).

What prevents Ca_v2.2 from undergoing CDF is unknown but may involve unique sequence elements in the CTD of the α_1 subunit based on analyses of Ca_v2.1 splice variants. Alternative splicing of exons in the proximal or distal CTD of the Ca_v2.1 α_1 subunit (exons 37 and 47, respectively; Fig. 1) gives rise to channels with

altered CDF (Chaudhuri et al., 2004). Notably, the corresponding exons of Ca_v2.2 also undergo alternative splicing with effects on Ca_v2.2 current density, modulation by G-proteins, and synaptic trafficking in neurons (Maximov and Bezprozvanny, 2002; Bell et al., 2004; Lipscombe et al., 2013). The potential of these alternatively spliced exons to regulate CDF of Ca_v2.2 has not been investigated.

In this study, we tested whether sequences encoded by exons 37 and 46, as well as other regions of the CTD, underlie the absence of CDF in Ca_v2.2. We find that although splice variation of exons 37 and 46 was inconsequential, the transfer of the key CDF regulatory sites in Ca_v2.1 to Ca_v2.2 unmasked strong CDF in the chimeric channels. However, transfer of any of these sites alone was ineffective. Our results reveal an unexpected variance in the molecular determinants controlling CaM regulation of Ca_v2.1 and Ca_v2.2, which may shape the

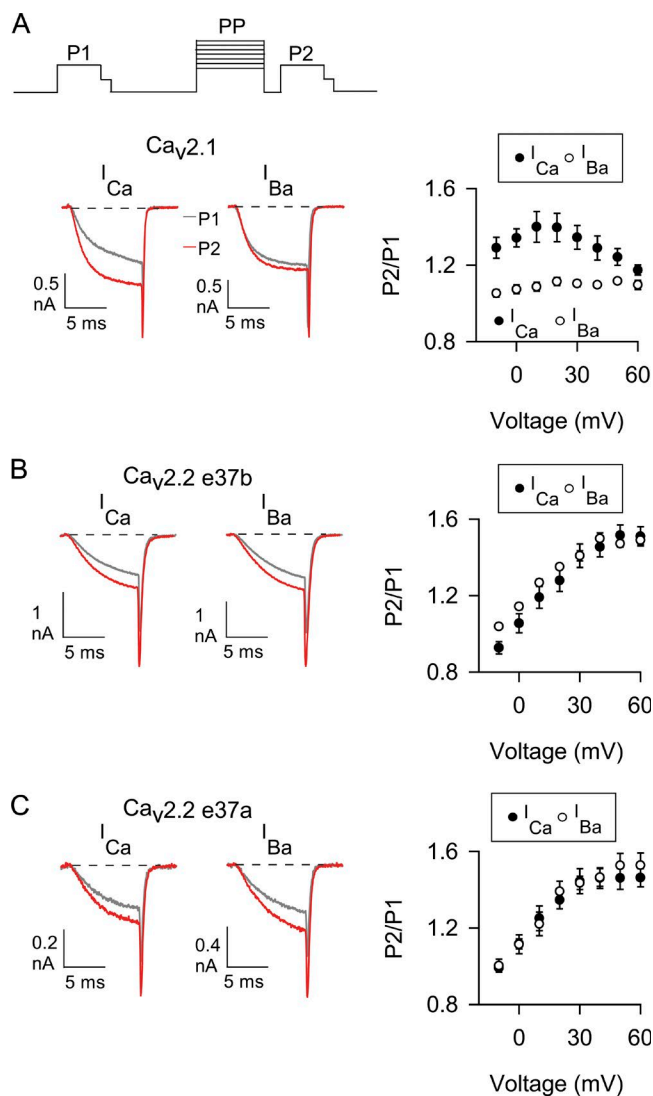


Figure 2. The absence of CDF in $Ca_v2.2$ is not affected by alternative splicing of exon 37. (A–C) Left, representative I_{Ca} and I_{Ba} evoked before (P1, gray trace) and after (P2, red trace) a prepulse to 20 mV for $Ca_v2.1$ (A) and $Ca_v2.2$ variants with exon 37b (B) or exon 37a (C). Current traces were overlaid for comparison. Voltage protocol is shown above. P1 and P2 pulses were 10-ms steps from -80 mV to -5 mV (for I_{Ca}) or -10 mV (for I_{Ba}) 1 s before and 5 ms after, respectively, a 50-ms prepulse to various voltages. For P2 and P1, tail currents were resolved by repolarization to -60 mV for 2 ms before stepping to -80 mV. Right, the ratio of P2 and P1 tail currents is plotted against prepulse voltages for I_{Ca} and I_{Ba} . Numbers of cells for I_{Ca} and I_{Ba} are indicated in Table 1. Data represent mean \pm SEM.

distinct coupling of these channels to vesicle release at the synapse.

MATERIALS AND METHODS

cDNAs and molecular biology

The following cDNAs were used: $Ca_v2.1$ (NM_001127221), $Ca_v2.2$ e37a (AF055477), $Ca_v2.2$ e37b (NM_147141), β_{2A} (NM_053851), and $\alpha_2\delta-1$ (NM_000722.3). The plas-

mid for β_{2A} -CaM was a gift from I. Dick (University of Maryland, Baltimore, MD). Chimeras were constructed using NEBuilder HiFi DNA Assembly Cloning System (New England Biolabs) and $Ca_v2.1$ and $Ca_v2.2$ e37a as templates. The following constructs were generated by swapping the amino acids indicated in parentheses: $Ca_v2.2$ -CT_{2.1}, $Ca_v2.1$ -CT_{2.2} (1,681–2,334 of $Ca_v2.2$, 1,786–2,261 of $Ca_v2.1$); $Ca_v2.2$ -EF_{2.1}, $Ca_v2.1$ -EF_{2.2} (1,681–1,788 of $Ca_v2.2$, 1,786–1,892 of $Ca_v2.1$); $Ca_v2.2$ -pre-IQ-IQ_{2.1}, $Ca_v2.1$ -pre-IQ-IQ_{2.2} (1,789–1,875 of $Ca_v2.2$, 1,893–1,985 of $Ca_v2.1$); and $Ca_v2.2$ -CBD_{2.1}, $Ca_v2.1$ -CBD_{2.2} (1,912–1,990 of $Ca_v2.2$, 2,009–2,084 of $Ca_v2.1$). Additional chimeric channels containing subsets of the EF-hand, pre-IQ, IQ, and CBD were generated using the residues indicated above. For $Ca_v2.2$ Δ e46, the sequence encoding exons 42–45 of $Ca_v2.2$ (1,927–2,162) followed by a stop codon was amplified by PCR and cloned into the corresponding site of $Ca_v2.2$ as an XbaI fragment. All chimeras and $Ca_v2.2$ Δ e46 constructs were cloned into the pcDNA6V5His vector. For generating glutathione S-transferase (GST) fusion proteins, sequences corresponding to the aforementioned Ca_v2 domains were amplified by PCR and cloned into BamHI and XhoI sites of the pGEX-4T-1 vector.

Cell culture and transfection

Human embryonic kidney 293 cells transformed with the SV40 T-antigen (HEK 293T, CRL-3216, RRID:CVCL_0063; ATCC) were maintained in Dulbecco's modified Eagle's medium with 10% FBS at 37°C in a humidified atmosphere with 5% CO₂. Cells were grown to 80% confluence and transfected using FuGene 6 (Promega) according to the manufacturer's protocol. Cells were plated in 35-mm dishes and transfected with cDNAs encoding Ca_v channel subunits (for $Ca_v2.1$ and chimeras with $Ca_v2.2$ CTDs: 1.0 μ g α_1 , 0.5 μ g β_{2A} , and 0.5 μ g $\alpha_2\delta_1$; for $Ca_v2.2$ and chimeras with $Ca_v2.1$ CTDs: 1.8 μ g α_1 , 0.6 μ g β_{2A} , and 0.6 μ g $\alpha_2\delta_1$). Cotransfection with cDNA encoding enhanced green fluorescent protein (pEGFP, 50 ng) allowed visualization of transfected cells.

Electrophysiological recordings

Whole-cell patch recordings were performed 24–72 h after transfection with a EPC-8 patch clamp amplifier and PatchMaster software (HEKA Elektronik). External recording solution contained (mM) 150 Tris, 1 MgCl₂, and 5 CaCl₂ or BaCl₂. Intracellular solution contained (mM) 140 N-methyl-D-glucamine, 10 HEPES, 10 or 0.5 EGTA, 2 MgCl₂, and 2 Mg-ATP. The pH of both solutions was adjusted to 7.3 using methanesulfonic acid. Electrode resistances were 4–6 M Ω in the bath solution. Series resistance was compensated 60–70%. Leak currents were subtracted using a P/–4 protocol. Data were analyzed using Igor Pro software (WaveMetrics). Averaged data represent mean \pm SEM and results from at least three independent transfections.

Table 1. F_{CDF} and P2/P1 for I_{Ca} and I_{Ba} from double-pulse protocol (20-mV prepulse)

Construct	P2/P1 for I_{Ca}	P2/P1 for I_{Ba}	P-value, I_{Ca} vs. I_{Ba} ^a	F_{CDF}	P-value vs. $Ca_v2.1$ ^b	P-value vs. $Ca_v2.2a$ ^b
$Ca_v2.1$	1.40 ± 0.07 (5)	1.11 ± 0.02 (7)	0.002	0.28 ± 0.07 (5)		0.032
$Ca_v2.2$ e37b	1.28 ± 0.06 (10)	1.35 ± 0.01 (5)	0.437	-0.07 ± 0.06 (10)	0.015	1.000
$Ca_v2.2$ e37a	1.39 ± 0.06 (8)	1.38 ± 0.04 (6)	0.232	0.01 ± 0.06 (7)	0.032	
$Ca_v2.2$ -CT _{2.1}	1.65 ± 0.10 (13)	1.32 ± 0.04 (11)	0.009	0.33 ± 0.10 (13)	1.000	0.019
$Ca_v2.1$ -CT _{2.2}	1.16 ± 0.10 (4)	1.16 ± 0.02 (5)	0.717	0.00 ± 0.10 (4)	0.035	1.000

F_{CDF} and P2/P1 (mean ± SEM) were determined as indicated in the text. Number of cells in parentheses.

^aDetermined by Student's *t* test.

^bDetermined by Kruskal-Wallis test and post-hoc Dunn's test.

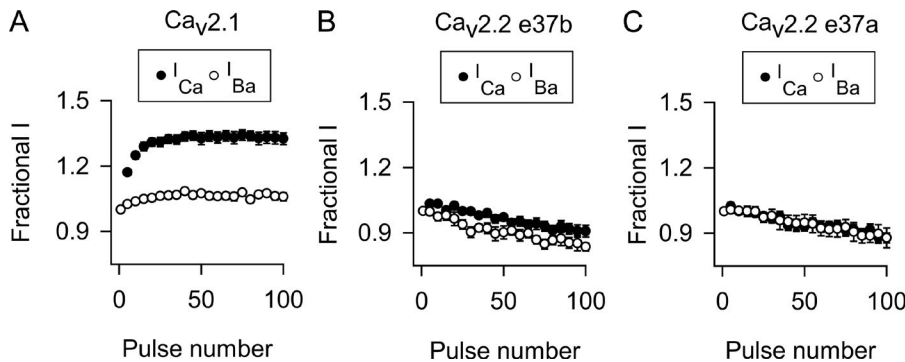


Figure 3. Repetitive depolarizations cause CDF for $Ca_v2.1$ but not $Ca_v2.2$. (A–C) I_{Ca} or I_{Ba} were evoked by 2-ms steps from -80 mV to 0 mV for I_{Ca} or -10 mV for I_{Ba} at 100 Hz in cells transfected with $Ca_v2.1$ (A) or $Ca_v2.2$ containing exon 37b (B) or exon 37a (C). The amplitude of each current was normalized to the first current of the train and plotted against pulse number. For clarity, every fifth point is plotted. Numbers of cells for I_{Ca} and I_{Ba} are indicated in Table 2. Data represent mean ± SEM.

Pull-down binding assays

The cDNA encoding full-length rat CaM (rCaM1-148 [Pedigo and Shea, 1995], provided by M. Shea) was expressed in BL21 DE3 *Escherichia coli* bacteria and purified as described previously (Theoharis et al., 2008). Purified CaM (1–10 µg) was added to GST or GST-tagged $Ca_v2.1$ or $Ca_v2.2$ proteins (5 µg) immobilized on glutathione Sepharose beads (GE Healthcare Life Sciences). The reaction was brought to a total volume of 750 µl with binding buffer (20 mM Tris-HCl, pH 7.3, 2 mM $CaCl_2$, ± 150 mM NaCl; results were similar with or without the added NaCl and so were combined). Binding reactions were incubated at 4°C, rotating for 1 h. The beads were washed three times with 1 ml ice-cold binding buffer, and bound proteins were eluted, resolved by SDS-PAGE, and transferred to nitrocellulose. To detect the GST-proteins, the nitrocellulose was first stained with Ponceau S. Bound CaM was then detected by Western blot with rabbit polyclonal antibodies against

CaM (1:1,000, 301 003, RRID:AB_2620046; Synaptic Systems). Blots were processed with HRP-conjugated secondary antibodies (anti-rabbit IgG, 1:4,000, I5006, RRID: AB_1163659; Sigma-Aldrich) and reagents for enhanced chemiluminescent detection (Thermo Fisher Scientific) before autoradiography.

For quantitative analysis, densitometry was performed using a Canon LIDE 200 scanner and ImageJ (NIH) software. The Western blot signal for CaM was normalized to the signal corresponding to the Ponceau-stained GST fusion proteins. Results from at least three independent experiments were pooled for statistical analysis.

Data presentation and statistical analysis

Data were incorporated into figures using SigmaPlot (Systat Software) and Adobe Illustrator software. Statistical analysis was performed with SigmaPlot or GraphPad Prism software. The data were first analyzed for

Table 2. F_{CDF} calculated from F_{96-100} for I_{Ca} and I_{Ba} from 100-Hz protocol

Construct	F_{96-100} for I_{Ca}	F_{96-100} for I_{Ba}	P-value, I_{Ca} vs. I_{Ba} ^a	F_{CDF}	P-value vs. $Ca_v2.1$ ^b	P-value vs. $Ca_v2.2a$ ^b
$Ca_v2.1$	1.33 ± 0.03 (10)	1.06 ± 0.02 (12)	<0.001	0.27 ± 0.03 (10)		<0.001
$Ca_v2.2$ e37b	0.91 ± 0.03 (10)	0.83 ± 0.02 (11)	0.067	0.07 ± 0.03 (10)	<0.001	0.360
$Ca_v2.2$ e37a	0.89 ± 0.02 (10)	0.88 ± 0.04 (10)	0.970	-0.01 ± 0.02 (10)	<0.001	
$Ca_v2.2$ e37a Δ46 (10 mM)	0.95 ± 0.03 (12)	0.83 ± 0.03 (10)	0.005	0.12 ± 0.03 (12)	0.002	0.028
$Ca_v2.2$ e37a Δ46 (0.5 mM)	0.82 ± 0.04 (10)	0.82 ± 0.03 (10)	0.968	0.00 ± 0.04 (10)	<0.001	1.000
$Ca_v2.2$ e37b Δ46 (10 mM)	0.94 ± 0.03 (8)	0.94 ± 0.02 (4)	0.985	0.00 ± 0.03 (8)	<0.001	1.000
$Ca_v2.2$ e37b Δ46 (0.5 mM)	0.86 ± 0.04 (5)	0.88 ± 0.02 (5)	0.646	-0.02 ± 0.04 (5)	<0.001	0.985

F_{CDF} and F_{96-100} (mean ± SEM) were determined as indicated in the text. Number of cells in parentheses.

^aDetermined by Student's *t* test.

^bDetermined by one-way ANOVA test and post-hoc Dunnett's test.

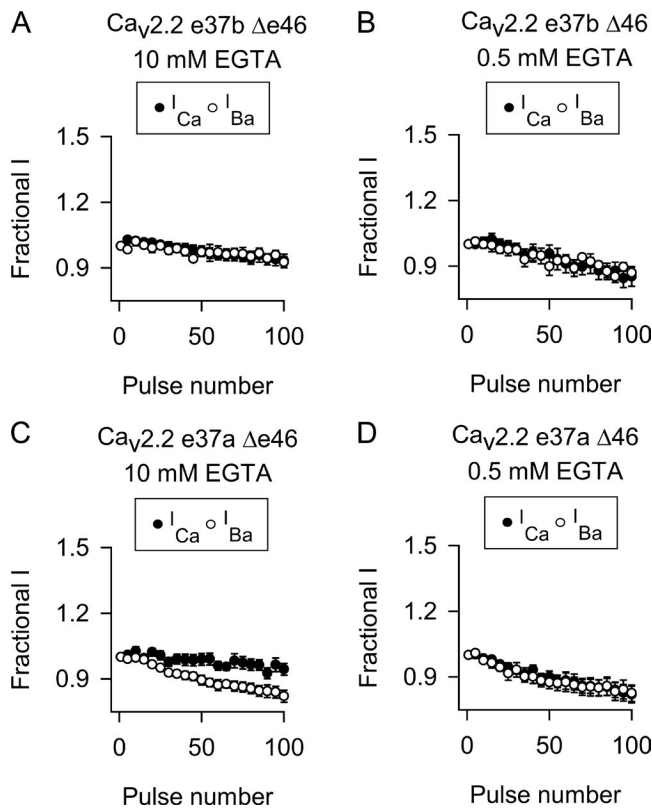


Figure 4. Deletion of exon 46 does not influence the absence of CDF in $Ca_v2.2$. (A–D) As in Fig. 3 except cells transfected with $Ca_v2.2$ e37b (A and B) or $Ca_v2.2$ e37a (C and D) without exon 46. The intracellular recording solution contained 10 or 0.5 mM EGTA as indicated. Data represent mean \pm SEM.

normality using the Shapiro–Wilk test. For parametric data, significant differences were determined by Student’s *t* test or ANOVA with post hoc Dunnett or Tukey test. For nonparametric data, Kruskal–Wallis and post hoc Dunn’s tests were used.

Online supplemental material

Effects of varying EGTA concentration in the intracellular recording solution are presented in Fig. S1. Fig. S2 shows that enrichment of local CaM does not produce CDF of $Ca_v2.1$ -EF-pre-IQ- $IQ_{2,2}$ or $Ca_v2.2$ e37a.

RESULTS

Effects of alternative splicing on CDF of $Ca_v2.2$

In both $Ca_v2.1$ and $Ca_v2.2$, exon 37 encodes a portion of an EF-hand-like (EF) domains similar to those found in a variety of Ca^{2+} binding proteins (Kawasaki and Kretsinger, 1995). Conserved in the proximal CTD of all Ca_v1 and Ca_v2 channels, the EF domain has been implicated in the regulation of CDI and Mg^{2+} -dependent inhibition of $Ca_v1.2$ channels (Peterson et al., 2000; Kim et al., 2004; Brunet et al., 2005). Alternative splicing of exon 37 gives rise to two $Ca_v2.1$ variants with distinct

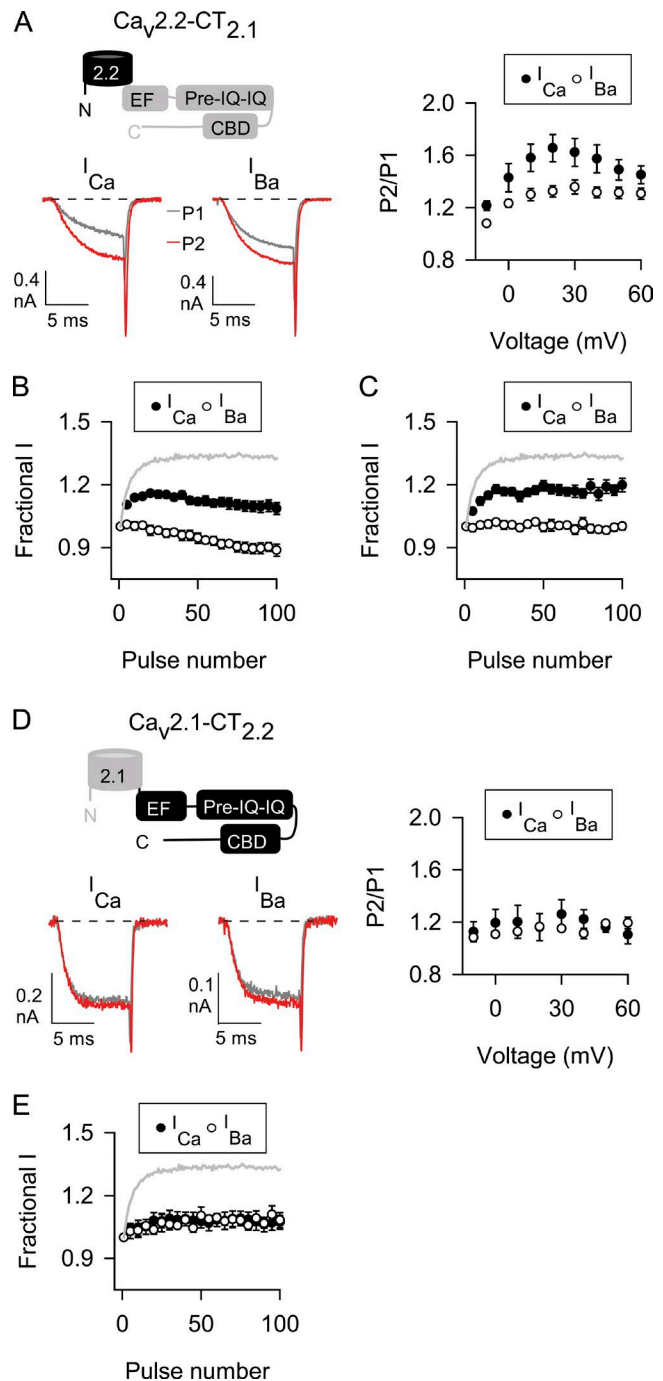


Figure 5. The CTDs of $Ca_v2.1$ and $Ca_v2.2$ distinguish their abilities to undergo CDF. (A–E) As in Fig. 2 (double-pulse protocol) and Fig. 3 (100-Hz protocol) except cells transfected with $Ca_v2.2$ channels with the CTD of $Ca_v2.1$ (A–C) or $Ca_v2.1$ channels with the CTD of $Ca_v2.2$ (D and E). In C, interpulse voltage was -140 mV. Gray line representing strong CDF of $Ca_v2.1$ I_{Ca} (from Fig. 3 A) is overlaid for comparison. Data represent mean \pm SEM.

EF domains (Fig. 1), but only channels containing one of the exons (exon 37a) exhibits strong CDF (Chaudhuri et al., 2004). The alternatively spliced exons 37a and 37b in $Ca_v2.2$ (Bell et al., 2004) are similar in se-

Table 3. F_{CDF} calculated from F_{96-100} for I_{Ca} and I_{Ba} from 100-Hz protocol

Construct	F_{96-100} for I_{Ca}	F_{96-100} for I_{Ba}	P-value, I_{Ca} vs. I_{Ba} ^a	F_{CDF}	P-value vs. Ca _v 2.1 ^b	P-value vs. Ca _v 2.2a ^b
Ca _v 2.2-CT _{2.1}	1.09 ± 0.03 (15)	0.89 ± 0.03 (15)	<0.001	0.20 ± 0.03 (15)	1.000	
Ca _v 2.2-pCT _{2.1}	1.07 ± 0.02 (13)	0.93 ± 0.02 (11)	<0.001	0.14 ± 0.02 (13)	0.370	
Ca _v 2.2-dCT _{2.1}	0.90 ± 0.03 (8)	0.92 ± 0.02 (10)	0.914	0.02 ± 0.03 (8)	<0.001	
Ca _v 2.2-EF _{2.1}	0.85 ± 0.03 (10)	0.88 ± 0.03 (10)	0.520	-0.03 ± 0.03 (10)	<0.001	
Ca _v 2.2-pre-IQ-IQ _{2.1}	0.90 ± 0.03 (10)	0.92 ± 0.02 (12)	0.583	-0.02 ± 0.03 (10)	<0.001	
Ca _v 2.2-CBD _{2.1}	0.99 ± 0.03 (10)	0.93 ± 0.02 (11)	0.149	0.06 ± 0.03 (10)	0.006	
Ca _v 2.2-pre-IQ-IQ-CBD _{2.1}	0.95 ± 0.02 (11)	0.95 ± 0.04 (6)	0.689	0.00 ± 0.02 (11)	<0.001	
Ca _v 2.2-EF&CBD _{2.1}	0.89 ± 0.03 (12)	0.86 ± 0.02 (10)	0.508	0.03 ± 0.03 (12)	0.001	
Ca _v 2.2-EF-pre-IQ-IQ _{2.1}	1.07 ± 0.03 (18)	0.94 ± 0.03 (13)	0.004	0.13 ± 0.03 (18)	0.851	
Ca _v 2.1-CT _{2.2}	1.08 ± 0.04 (10)	1.08 ± 0.02 (5)	0.966	0.00 ± 0.04 (10)		1.000
Ca _v 2.1-pCT _{2.2}	1.05 ± 0.02 (5)	1.01 ± 0.02 (7)	0.073	0.04 ± 0.02 (5)		1.000
Ca _v 2.1-dCT _{2.2}	1.24 ± 0.03 (4)	1.02 ± 0.02 (3)	0.024	0.22 ± 0.03 (4)		0.054
Ca _v 2.1-EF _{2.2}	1.08 ± 0.03 (4)	1.02 ± 0.02 (6)	0.257	0.06 ± 0.03 (4)		1.000
Ca _v 2.1-pre-IQ-IQ _{2.2}	1.03 ± 0.01 (8)	1.03 ± 0.02 (6)	0.831	0.00 ± 0.02 (8)		1.000
Ca _v 2.1-CBD _{2.2}	1.27 ± 0.02 (8)	1.04 ± 0.04 (10)	<0.001	0.23 ± 0.02 (8)		0.005
Ca _v 2.1-EF-pre-IQ-IQ _{2.2}	1.05 ± 0.01 (11)	1.06 ± 0.02 (11)	0.645	-0.01 ± 0.00 (11)		1.000

F_{CDF} and F_{96-100} (mean ± SEM) were determined as indicated in the text. Number of cells in parentheses.

^aDetermined by Student's *t* test.

^bDetermined by Kruskal–Wallis test and post-hoc Dunn's test.

quence to the corresponding exons in Ca_v2.1 (Fig. 1). Notably, previous analysis of CDF in Ca_v2.2 used the variant containing exon 37b (Liang et al., 2003); the corresponding exon in long variants of Ca_v2.1 prevents CDF (Chaudhuri et al., 2004). Therefore, CDF may have been missed in the previous study (Liang et al., 2003) if exon 37a is required for CDF of Ca_v2.2.

We tested this possibility in whole-cell patch clamp recordings of transfected HEK 293T cells. To analyze CDF, we used a classic voltage protocol in which the amplitudes of currents evoked before (P1) and after (P2) a conditioning prepulse are compared (Thomas and Lee, 2016). The extracellular solution contained either Ca²⁺ or Ba²⁺, and the intracellular recording solution contained a high concentration of EGTA (10 mM), which blocks CDI while sparing CDF of Ca_v2 channels (Lee et al., 2000; Liang et al., 2003). With this protocol, Ca_v2.1 (containing exon 37a) exhibited the hallmarks of CDF: the ratio of P2 to P1 was greater for Ca²⁺ currents (I_{Ca}) than for Ba²⁺ currents (I_{Ba}) for most prepulse voltages (Fig. 2 A). Consistent with a role for Ca²⁺ influx during the prepulse in promoting CDF (Lee et al., 2000), the difference between P2/P1 for I_{Ca} and I_{Ba} was greatest at prepulse voltages evoking the peak inward I_{Ca} (20 mV) and was used as a metric for CDF (F_{CDF}). Similar to previous findings (Liang et al., 2003), Ca_v2.2 e37b did not undergo CDF, in that P2/P1 was similar for I_{Ca} and I_{Ba} across all prepulse voltages (Fig. 2 B) and F_{CDF} was nominal (Table 1). The P2/P1 ratio for both I_{Ca} and I_{Ba} increased monotonically with prepulse voltage (Fig. 2 B), likely because of voltage-dependent removal of basal G-protein inhibition (Li et al., 2004). F_{CDF} was not significantly different for Ca_v2.2 containing exons 37a or 37b (Fig. 2 C; and Table 1), which argued against this exon being permissive for CDF.

To determine whether CDF of the Ca_v2.2 splice variants might be revealed with more physiological stimuli, we analyzed I_{Ca} and I_{Ba} evoked by trains of depolarizations at 100 Hz. The amplitude of each current was normalized to that of the first pulse (Fractional I) and plotted against pulse number. As shown previously (Lee et al., 2000), I_{Ca} mediated by Ca_v2.1 undergoes a robust and sustained increase, whereas I_{Ba} undergoes relatively modest voltage-dependent facilitation during the train (Fig. 3 A). The mean of the last five pulses (F_{96-100}) was significantly greater for I_{Ca} than for I_{Ba} (~25%; Table 2), indicative of CDF. In contrast, there was no difference in F_{96-100} for I_{Ca} and I_{Ba} mediated by Ca_v2.2 e37a or e37b (Fig. 3, B and C; and Table 2). These results confirm that inclusion of exon 37a is insufficient to confer Ca_v2.2 channels with an ability to undergo CDF, in contrast to the role of the analogous exon in Ca_v2.1 (Chaudhuri et al., 2004).

For Ca_v2.1 channels, the insensitivity of CDF to high intracellular Ca²⁺ buffering arises from its dependence on local Ca²⁺ signals detected by the C-terminal lobe of CaM (Chaudhuri et al., 2007). In the context of exon 37b, deletion of exon 47 from Ca_v2.1 (Ca_v2.1 e37b Δe47) converts CDF to a reliance on global elevations in Ca²⁺, which are sensed by the N-terminal lobe of CaM and can be blunted by a high intracellular concentration of Ca²⁺ chelator (Chaudhuri et al., 2004). Therefore, we tested whether deletion of the analogous exon 46 of Ca_v2.2 e37b (Ca_v2.2e37b Δex46) might reveal CDF under conditions of limited Ca²⁺ buffering (0.5 mM EGTA). With this approach, there was no significant difference in I_{Ca} and I_{Ba} evoked by the 100-Hz protocol in cells transfected with Ca_v2.2e37b Δex46 with either 10 or 0.5 mM EGTA (Fig. 4, A and B; and Table 2). With 10 mM EGTA, deletion of exon 46 from Ca_v2.2e37a led to a small increase in the F_{96-100} for I_{Ca} at the end of the train compared with I_{Ba} , but F_{CDF} was nominal and significantly weaker than

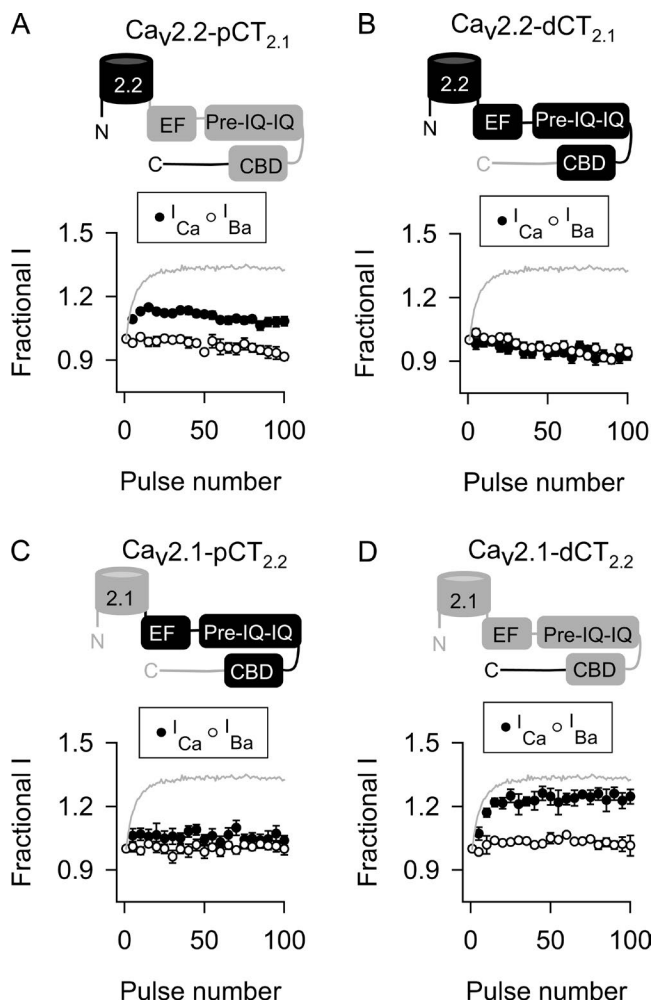


Figure 6. The proximal CTD containing CDF-regulatory domains in $Ca_v2.1$ is not functionally conserved in $Ca_v2.2$. (A–D) As in Fig. 5 B except cells transfected with $Ca_v2.2$ channels containing proximal (A) or distal (B) CTD or $Ca_v2.1$ channels containing proximal (C) or distal (D) CTD of $Ca_v2.2$. Data represent mean \pm SEM.

that for $Ca_v2.1$ (Fig. 4, C and D; and Table 2). Our strategy of manipulating the Ca^{2+} -dependent effects of CaM was effective in that strong inactivation of I_{Ca} caused by CDI with 0.5 mM EGTA was significantly reduced with 10 mM EGTA in the intracellular recording solution (Fig. S1). Collectively, our results show that alternative splicing of exons in the proximal and distal CTD do not account for the lack of CDF of $Ca_v2.2$.

Role of CaM-regulatory regions in CDF of Ca_v2 channels

Mutations of the IQ-like domain that inhibit CaM binding abolish CDF (DeMaria et al., 2001; Lee et al., 2003), whereas deletion of the CBD diminishes CDF and CDI (Lee et al., 1999, 2000, 2003). Although its role in CDF of $Ca_v2.1$ is not established, the pre-IQ domain upstream of the IQ domain also interacts with CaM and

regulates CDI and CDF of $Ca_v1.2$ channels (Pitt et al., 2001; Kim et al., 2004, 2010). Each of these domains is conserved in $Ca_v2.1$ and $Ca_v2.2$ (Fig. 1), but key differences in their amino acid sequences may allow CDF of $Ca_v2.1$ but not $Ca_v2.2$. If so, then CDF should be conferred to $Ca_v2.2$ upon transfer of the corresponding domains from $Ca_v2.1$. Consistent with this prediction, chimeric $Ca_v2.2$ channels containing the CTD of $Ca_v2.1$ ($Ca_v2.2-CT_{2.1}$; $Ca_v2.2a$ variant was used for all $Ca_v2.2$ chimeras) exhibited robust CDF with the double-pulse protocol, with F_{CDF} not significantly different from that of $Ca_v2.1$ channels (Fig. 5 A and Table 1).

With the 100-Hz protocol, F_{96-100} for $Ca_v2.2-CT_{2.1}$ I_{Ca} was not as great as that for $Ca_v2.1$ (Fig. 5 B and Tables 2 and 3) perhaps because of closed-state inactivation, which is prominent for $Ca_v2.2$ during repetitive depolarizations and relieved by hyperpolarized interpulse voltages (Patil et al., 1998). $Ca_v2.2$ inactivation (I_{Ca} and I_{Ba}) was stronger than that for $Ca_v2.1$ during 100-Hz trains (Fig. 3) and could partially occlude facilitation of $Ca_v2.2-CT_{2.1}$ I_{Ca} . Changing the interpulse voltage from -80 to -140 mV increased F_{96-100} for I_{Ca} (1.19 ± 0.03 for -140 mV, $n = 10$, vs. 1.09 ± 0.03 for -80 mV, $n = 15$, $P = 0.013$ by t test) to a similar extent as for I_{Ba} ($F_{96-100} = 0.99 \pm 0.02$ for -140 mV, $n = 10$, vs. 0.89 ± 0.03 for -80 mV, $n = 15$, $P = 0.014$ by t test; Fig. 5 C), such that F_{CDF} was similar regardless of interpulse voltage (0.21 ± 0.03 for -140 mV, $n = 10$, vs. 0.20 ± 0.03 for -80 mV, $n = 15$, $P = 0.926$ by t test; Fig. 5 C). Thus, although closed-state inactivation does indeed underlie the smaller F_{96-100} for $Ca_v2.2-CT_{2.1}$ I_{Ca} compared with $Ca_v2.1$ I_{Ca} , it does not affect the magnitude of CDF. In fact, F_{CDF} of $Ca_v2.2-CT_{2.1}$ was not significantly different from that for $Ca_v2.1$ (Table 3). Collectively, our results indicate that molecular determinants within the CTD of $Ca_v2.1$ are sufficient to enable $Ca_v2.2-CT_{2.1}$ to undergo CDF.

We next tested the converse prediction that transfer of the $Ca_v2.2$ CTD to $Ca_v2.1$ should blunt CDF. In contrast to the wild-type $Ca_v2.1$, I_{Ca} and I_{Ba} behaved similarly in double-pulse and 100-Hz protocols in cells transfected with the chimeric $Ca_v2.1-CT_{2.1}$ channels (Fig. 5, D and E; and Tables 1 and 3). To further refine the molecular determinants in the CTD responsible for “turning off” $Ca_v2.2$ CDF, we analyzed additional chimeric channels. For these studies, data are shown only for the 100-Hz protocol because similar results were obtained with double-pulse protocols. If the CDF-regulatory domains of $Ca_v2.1$ and $Ca_v2.2$ distinguish their abilities to undergo CDF, $Ca_v2.2$ channels containing the proximal CTD ($Ca_v2.2-pCT_{2.1}$) but not the distal CTD ($Ca_v2.2-dCT_{2.1}$) should exhibit CDF. As expected, $Ca_v2.2-pCT_{2.1}$ underwent CDF (Fig. 6 A and Table 3). In contrast, $Ca_v2.2-dCT_{2.1}$ was similar to wild-type $Ca_v2.2$ in that there was no difference in F_{96-100} for I_{Ca} and I_{Ba} (Fig. 6 B and Table 3). Consistent with these findings, transfer of the proximal CTD but not the distal CTD

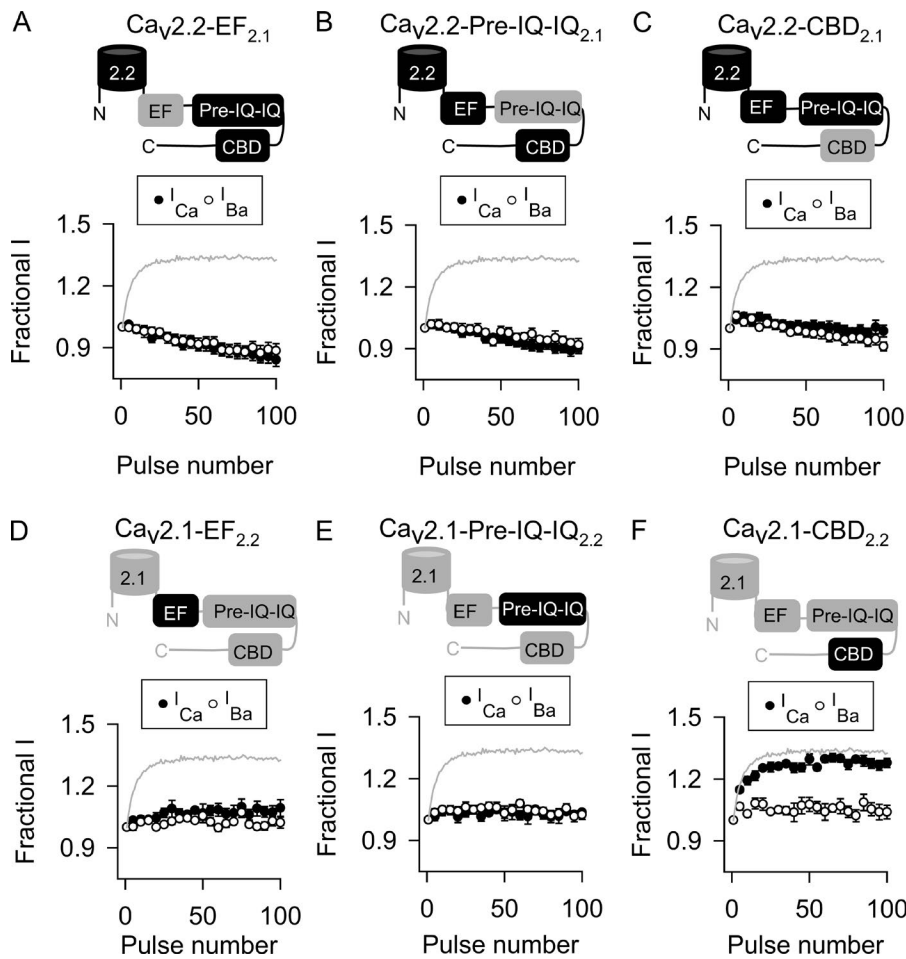


Figure 7. EF-hand and pre-IQ-IQ domains are the minimal determinants in the CTD that disable CDF in Ca_v2.2. (A–F) As in Fig. 5 B except cells transfected with Ca_v2.2 channels containing EF-hand, pre-IQ-IQ, or CBD of Ca_v2.1 (A–C) or Ca_v2.1 channels containing corresponding regions of Ca_v2.2 (D–F). Data represent mean ± SEM.

of Ca_v2.2 to Ca_v2.1 resulted in chimeric channels that did not undergo CDF (Fig. 6, C and D; and Table 3). Therefore, the proximal CTD contains the sequence elements that distinguish the ability of Ca_v2.1 and Ca_v2.2 to undergo CDF.

We next determined the relative contributions of the EF, pre-IQ, IQ, and CBDs in disabling CDF in Ca_v2.2 channels. In these experiments, the pre-IQ and IQ sequences were transferred together because they work in concert to transduce effects of CaM in Ca_v1.2 (Pitt et al., 2001; Kim et al., 2004). None of the Ca_v2.2 chimeras containing these domains from Ca_v2.1 exhibited CDF (Fig. 7, A–C; and Table 3), indicating that the individual CDF-regulatory sites in Ca_v2.1 are dysfunctional within the context of the Ca_v2.2 proximal CTD. At the same time, substitution of the pre-IQ-IQ or EF-hand domain, but not the CBD, of Ca_v2.2 into Ca_v2.1 abolished CDF normally observed for the wild-type Ca_v2.1 (Fig. 7, D–F; and Table 3). Collectively, these results suggested that functional differences primarily in the EF-hand and pre-IQ-IQ domain of Ca_v2.2 prevent CDF. To test this, we analyzed chimeric Ca_v2.2 channels containing subsets of the CDF-regulatory sites in Ca_v2.1. Of these, only the Ca_v2.2 chimera containing the EF-hand and pre-IQ-IQ domain (EF-pre-IQ-IQ) of Ca_v2.1 exhibited

CDF (Fig. 8, A–C; and Table 3). Conversely, CDF was abolished in Ca_v2.1 channels containing the Ca_v2.2 EF-pre-IQ-IQ domain (Fig. 8 D and Table 3).

The inability of EF-pre-IQ-IQ to support CDF in Ca_v2.2 could be caused by weaker interactions with CaM compared with this region in Ca_v2.1. Indeed, past work suggests that CaM binds with lower affinity to the pre-IQ and IQ regions of Ca_v2.2 than of Ca_v2.1 (Peterson et al., 1999; Liang et al., 2003). To test whether this is the case in the context of EF-pre-IQ-IQ, we compared binding to GST-tagged Ca_v2.1 or Ca_v2.2 fusion proteins in pull-down assays. Consistent with previous results (Liang et al., 2003), CaM binding was significantly stronger to the pre-IQ-IQ of Ca_v2.1 than to this region of Ca_v2.2 or the GST control (Fig. 9, A and B). Remarkably, addition of the EF-hand to the pre-IQ-IQ of Ca_v2.2 greatly enhanced the interaction with CaM such that there was no significant difference in CaM binding to the EF-pre-IQ-IQ domain of Ca_v2.2 and Ca_v2.1 (Fig. 9, A and B). In contrast, CaM bound equally well to the pre-IQ-IQ and EF-pre-IQ-IQ domains of Ca_v2.1 (Fig. 9, A and B). The impact of the EF-hand on CaM binding to the Ca_v2.2 pre-IQ-IQ was particularly apparent with increasing amounts of CaM added to the binding reactions. For all concentrations of CaM tested, the amount of CaM

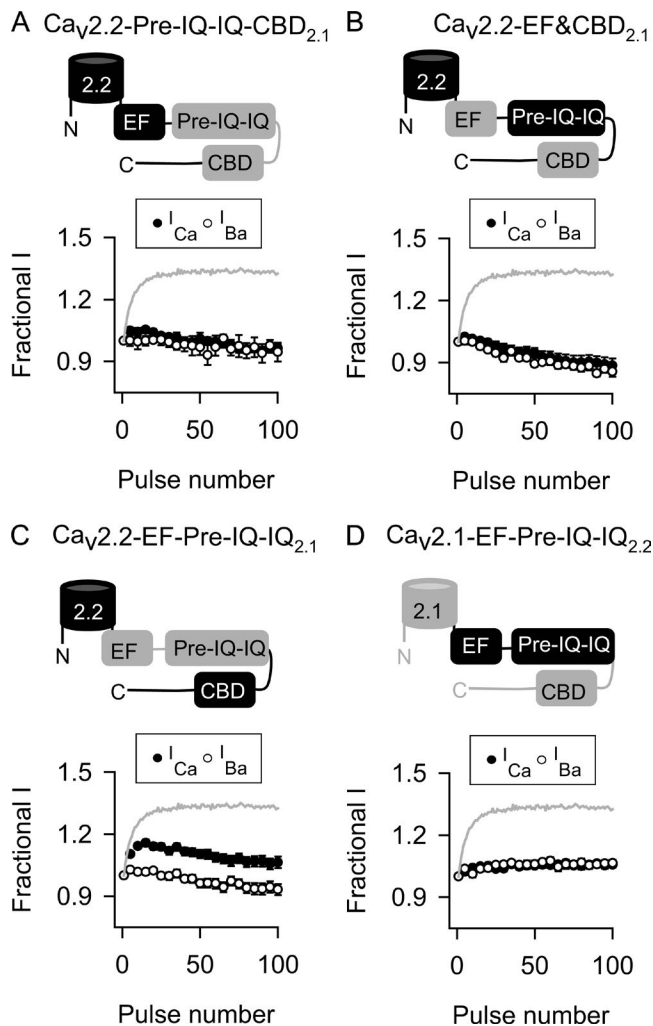


Figure 8. Both EF-hand and pre-IQ-IQ domains of $Ca_v2.1$ are required to unmask CDF in $Ca_v2.2$. (A–D) As in Fig. 5 B except cells transfected with $Ca_v2.2$ channels containing pre-IQ-IQ and CBD (A), EF-hand and CBD (B), or EF-hand and pre-IQ-IQ (C) of $Ca_v2.1$ or $Ca_v2.2$ channels containing EF-hand and pre-IQ-IQ of $Ca_v2.1$ (D). Data represent mean \pm SEM.

bound to the $Ca_v2.2$ pre-IQ-IQ was only $\sim 20\%$ of that to the $Ca_v2.1$ pre-IQ-IQ (Fig. 9, C and D) whereas there was no difference in CaM binding to the EF-pre-IQ-IQ of the two channels (Fig. 9, E and F).

The similar CaM binding abilities of the EF-pre-IQ-IQ domain of $Ca_v2.1$ and $Ca_v2.2$ suggested that the lack of CDF in $Ca_v2.2$ channels does not simply result from reduced affinity for CaM. If so, then increasing the concentration of CaM to overcome any such differences in CaM binding affinity between $Ca_v2.1$ and $Ca_v2.2$ should not uncover CDF. To test this prediction, we used a strategy to enrich the local concentration of CaM near Ca_v channels in which CaM is tethered to the auxiliary $Ca_v\beta_{2a}$ subunit (β_{2a} -CaM; Sang et al., 2016). Using β_{2a} as a control, we analyzed the effects of β_{2a} -CaM on the amplitude of I_{Ca} evoked by 100-Hz stimuli in cells cotransfected with $Ca_v2.2$ or $Ca_v2.1$ chimeras contain-

ing the EF-pre-IQ-IQ domain of $Ca_v2.2$ ($Ca_v2.1$ -EF-pre-IQ-IQ_{2.2}). Coexpression of β_{2a} -CaM (verified by Western blots) had no effect on I_{Ca} : CDF was not rescued in $Ca_v2.1$ -EF-pre-IQ-IQ_{2.2}, nor was it uncovered in $Ca_v2.2$ (Fig. S2). We conclude that the lack of CDF shown by $Ca_v2.2$ channels does not arise from weaker binding of CaM, but likely through an inability of the EF-pre-IQ-IQ domain to convert CaM binding into channel conformations that support CDF.

DISCUSSION

In this study, we uncovered new insights into the molecular determinants regulating CDF of Ca_v2 channels. First, we discounted a role for alternatively spliced C-terminal exons 37 and 46. Inclusion of exon 37a, which is permissive for CDF in $Ca_v2.1$ (Chaudhuri et al., 2004), did not reveal CDF in $Ca_v2.2$ (Figs. 2 and 3), nor did deletion of exon 46 (Fig. 4), which influences the Ca^{2+} dependence of $Ca_v2.1$ CDF (Chaudhuri et al., 2004). Second, we identified the EF-hand and pre-IQ-IQ domains as the critical determinants distinguishing the abilities of $Ca_v2.1$ and $Ca_v2.2$ to undergo CDF. These domains in the proximal CTD of $Ca_v2.2$ functionally diverge from those in $Ca_v2.1$ because their transfer to $Ca_v2.1$ prevented CDF (Fig. 6 C). Third, we discovered an unexpected role for the EF-hand domain in strengthening the ability of the pre-IQ-IQ of $Ca_v2.2$ to bind CaM. Our results support a model in which CaM binds to the EF-pre-IQ-IQ of $Ca_v2.2$ in a way that is functionally uncoupled from CDF.

The importance of the IQ domain for CDF is demonstrated by findings that mutation of the initial isoleucine and glutamine in the $Ca_v2.1$ IQ domain diminishes CaM binding and blunts CDF (DeMaria et al., 2001; Lee et al., 2003). Although the IQ domain is highly conserved in Ca_v1 and Ca_v2 channels, sequence alterations between Ca_v subtypes could underlie functional differences in channel regulation by CaM. By x-ray crystallography, Kim et al. (2008) found subtle differences in how CaM interacts with peptides corresponding to the IQ domain $Ca_v2.2$ and $Ca_v2.1$. These differences include less contact with the methionine at position -1 and greater interaction with phenylalanine at position 1 relative to the central isoleucine (position 0; Kim et al., 2008). These alterations may account for weaker CaM binding to the IQ and pre-IQ-IQ of $Ca_v2.2$ compared with $Ca_v2.1$ (Fig. 9; DeMaria et al., 2001; Liang et al., 2003). However, they are not sufficient to explain the absence of CDF in $Ca_v2.2$ channels because transfer of the $Ca_v2.1$ pre-IQ-IQ region alone to $Ca_v2.2$ did not reverse the inability of $Ca_v2.2$ to undergo CDF (Fig. 7 B). Moreover, $Ca_v2.3$ does not undergo CDF, and yet the crystal structures of CaM bound to the $Ca_v2.1$ and $Ca_v2.3$ IQ domains are nearly identical (Kim et al., 2008; Mori et al., 2008).

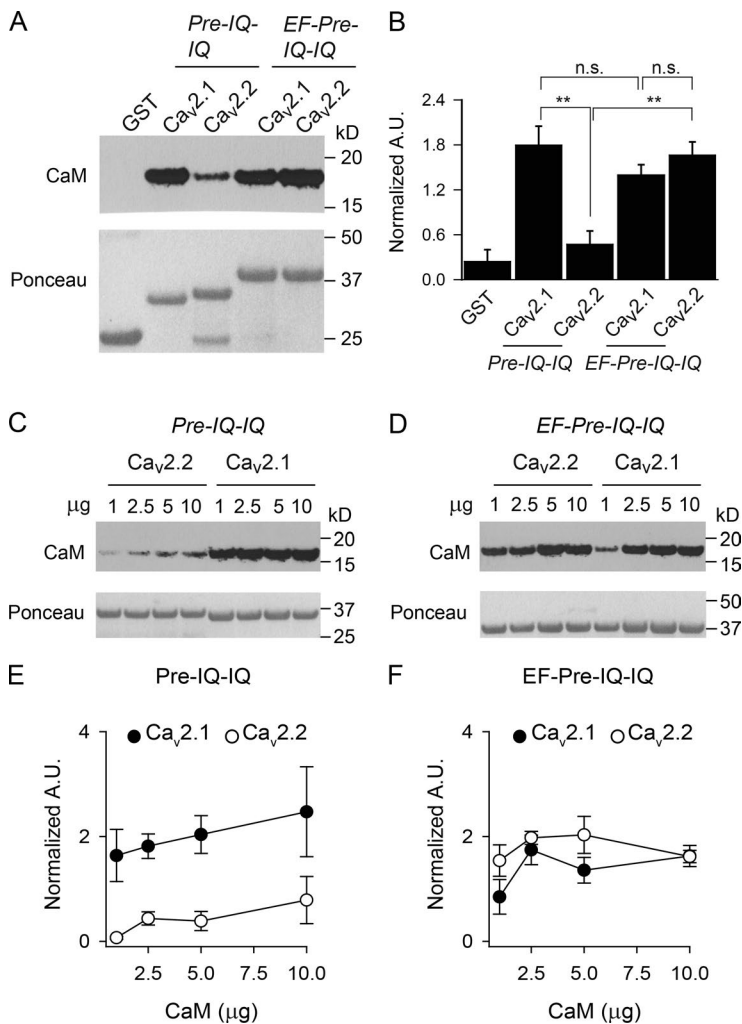


Figure 9. CaM differentially interacts with pre-IQ-IQ and EF-pre-IQ-IQ of Ca_v2.1 and Ca_v2.2 in pull-down assays. (A and B) GST or GST-tagged Ca_v2 proteins were incubated with CaM (2.5 μg), and bound CaM was detected by Western blotting. Ponceau staining indicated the amount of each GST protein in the reactions. In B, the signal intensity corresponding to CaM was normalized to that for the GST-protein. A.U., arbitrary units; n.s., not significant; **, P < 0.001, one-way ANOVA and post hoc Tukey test. Data are representative of four independent experiments. (C–F) As in A and B except that variable amounts of CaM (1–10 μg) were used in the assay. In E and F, data were analyzed by two-way ANOVA. There was a significant difference in results obtained for pre-IQ-IQ (P < 0.01) but not EF-pre-IQ-IQ (P = 0.75) of Ca_v2.1 and Ca_v2.2. Data are representative of three independent experiments. Data represent mean ± SEM.

In this context, the crystal structure presented by Kim et al. (2010) of CaM in complex with the Ca_v1.2 pre-IQ-IQ may be informative. The structure indicates a 2:1 stoichiometry with one Ca²⁺/CaM bound to the IQ domain and a second to a lower-affinity site in the pre-IQ region. A key tryptophan residue in the Ca_v1.2 pre-IQ region was identified as an anchoring site for the C-terminal lobe of CaM, and the mutation of this residue disrupted CDF when the initial isoleucine in the IQ-domain was also mutated so as to disrupt CDI (Kim et al., 2010). This tryptophan is conserved among all Ca_v1 and Ca_v2 channels and therefore may serve as an analogous region for binding Ca²⁺/CaM in Ca_v2 channels. Differences between the pre-IQ region of Ca_v2.1 and Ca_v2.2 include residues at positions –3, –4, and –12 from this tryptophan, which are all methionines in Ca_v2.1. Such differences could prevent the ability of CaM bound to the pre-IQ to produce CDF in Ca_v2.2, which would explain the absence of CDF in any of the Ca_v2.1 chimeras containing the Ca_v2.2 pre-IQ-IQ (Fig. 5, D and E; Fig. 6 C; and Fig. 7 E).

Considering the weak binding of CaM to the pre-IQ-IQ of Ca_v2.2 (Fig. 9; DeMaria et al., 2001; Liang et

al., 2003), the equivalence of CaM binding of the EF-pre-IQ-IQ of Ca_v2.2 and Ca_v2.1 (Fig. 9) suggests that the EF-hand domain differentially regulates interactions with CaM in the two channels. This is surprising given the strong sequence conservation in the EF-hand domains of Ca_v2.1 and Ca_v2.2 (Fig. 1). The divergent residues in the Ca_v2.2 EF-hand may be significant enough to facilitate interaction of CaM with the pre-IQ-IQ in ways that are unnecessary for Ca_v2.1. The Ca_v2.2 EF-hand might reposition CaM bound to the pre-IQ-IQ so as to prevent CDF, which could explain the absence of CDF in the Ca_v2.1 chimera containing the Ca_v2.2 EF-hand (Fig. 7 D). Alternatively, interactions of the EF-pre-IQ-IQ with other parts of the channel such as the cytoplasmic loops linking domains I and II (Kim et al., 2004) and III and IV (Wu et al., 2016) may be unfavorable for entry of Ca_v2.2 into the facilitated state that is normally triggered by Ca²⁺/CaM in Ca_v2.1.

Although it binds CaM and regulates CDI of Ca_v2.1 (Lee et al., 1999, 2000), the CBD plays a more modulatory role and works with the IQ domain to promote CDF (Lee et al., 2003). This is supported by our findings that Ca_v2.2 channels containing only the Ca_v2.1

CBD were unable to undergo CDF (Fig. 7 C). Only when cotransferred with the Ca_v2.1 EF-hand and pre-IQ-IQ domain was the Ca_v2.1 CBD effective in producing CDF in Ca_v2.2 (Figs. 5 A and 6 D). The CBD may be functionally redundant in Ca_v2.1 and Ca_v2.2, because CDF in Ca_v2.1 channels containing the Ca_v2.2 CBD was comparable to that in WT Ca_v2.1 channels (Fig. 7 F). Considering that CDF was slightly weaker in Ca_v2.2-pCT_{2.1} than Ca_v2.2-CT_{2.1} (Table 3), it may be that the CBD requires the distal CTD of Ca_v2.1 to fully promote CDF. An understanding of how the EF-hand, pre-IQ-IQ, and CBD domains coordinately regulate CDF is an important challenge for future studies.

The neurophysiological importance of disabling CDF in Ca_v2.2 channels is not entirely clear but may relate to the major roles of these channels in the peripheral nervous system (Hirning et al., 1988). Localized in the presynaptic terminals of small-diameter nociceptive neurons, Ca_v2.2 channels mediate the release of neuropeptides into the superficial layers of the spinal dorsal horn in response to painful stimuli (Holz et al., 1988; Maggi et al., 1990). Because the amount of neurotransmitter released is proportional to the third or fourth power of the presynaptic Ca²⁺ concentration (Dodge and Rahamimoff, 1967; Sakaba and Neher, 2001), the inability of Ca_v2.2 to undergo Ca²⁺/CaM-dependent CDF may have evolved to limit additive effects with other forms of Ca_v2.2 modulation that could collectively exacerbate transmission of painful stimuli. For example, Ca_v2.2 channel spinal nociceptive neurons undergo a CaMKII-dependent longer-term CDF that is eliminated with peripheral nerve injury (Tang et al., 2012). In sympathetic neurons, Ca_v2.2 channels are inhibited by a wide range of hormones and neurotransmitters acting via G protein-coupled receptors (Hille, 1994). If present in Ca_v2.2, CDF would oppose this inhibition, leading to improper neurohumoral control of sympathetic outflow.

ACKNOWLEDGMENTS

We thank Dr. Madeline Shea for providing guidance on CaM binding assays and Dr. Ivy Dick for providing the β_{2a}-CaM cDNA.

This work is supported by grants from the National Institutes of Health (NS084190, DC009433, and NS045549) and a Carver Research Program of Excellence Award.

The authors declare no competing financial interests.

Author contributions: J.R. Thomas, J. Hagen, and D. Soh conducted the research. All authors contributed to experimental design. J.R. Thomas and A. Lee wrote the paper.

Richard W. Aldrich served as editor.

Submitted: 26 June 2017

Revised: 29 September 2017

Accepted: 27 October 2017

REFERENCES

Bell, T.J., C. Thaler, A.J. Castiglioni, T.D. Helton, and D. Lipscombe. 2004. Cell-specific alternative splicing increases calcium channel

- current density in the pain pathway. *Neuron*. 41:127–138. [https://doi.org/10.1016/S0896-6273\(03\)00801-8](https://doi.org/10.1016/S0896-6273(03)00801-8)
- Boland, L.M., J.A. Morrill, and B.P. Bean. 1994. omega-Conotoxin block of N-type calcium channels in frog and rat sympathetic neurons. *J. Neurosci.* 14:5011–5027.
- Brunet, S., T. Scheuer, R. Klevit, and W.A. Catterall. 2005. Modulation of CaV1.2 channels by Mg²⁺ acting at an EF-hand motif in the COOH-terminal domain. *J. Gen. Physiol.* 126:311–323. <https://doi.org/10.1085/jgp.200509333>
- Catterall, W.A., K. Leal, and E. Nanou. 2013. Calcium channels and short-term synaptic plasticity. *J. Biol. Chem.* 288:10742–10749. <https://doi.org/10.1074/jbc.R112.411645>
- Chaudhuri, D., S.Y. Chang, C.D. DeMaria, R.S. Alvania, T.W. Soong, and D.T. Yue. 2004. Alternative splicing as a molecular switch for Ca²⁺/calmodulin-dependent facilitation of P/Q-type Ca²⁺ channels. *J. Neurosci.* 24:6334–6342. <https://doi.org/10.1523/JNEUROSCI.1712-04.2004>
- Chaudhuri, D., J.B. Issa, and D.T. Yue. 2007. Elementary mechanisms producing facilitation of Ca_v2.1 (P/Q-type) channels. *J. Gen. Physiol.* 129:385–401. <https://doi.org/10.1085/jgp.200709749>
- Cuttle, M.F., T. Tsujimoto, I.D. Forsythe, and T. Takahashi. 1998. Facilitation of the presynaptic calcium current at an auditory synapse in rat brainstem. *J. Physiol.* 512:723–729. <https://doi.org/10.1111/j.1469-7793.1998.723bd.x>
- DeMaria, C.D., T.W. Soong, B.A. Alseikhan, R.S. Alvania, and D.T. Yue. 2001. Calmodulin bifurcates the local Ca²⁺ signal that modulates P/Q-type Ca²⁺ channels. *Nature*. 411:484–489. <https://doi.org/10.1038/35078091>
- Dodge, F.A. Jr., and R. Rahamimoff. 1967. Co-operative action a calcium ions in transmitter release at the neuromuscular junction. *J. Physiol.* 193:419–432. <https://doi.org/10.1113/jphysiol.1967.sp008367>
- Dunlap, K., J.I. Luebke, and T.J. Turner. 1995. Exocytotic Ca²⁺ channels in mammalian central neurons. *Trends Neurosci.* 18:89–98. [https://doi.org/10.1016/0166-2236\(95\)80030-6](https://doi.org/10.1016/0166-2236(95)80030-6)
- Forsythe, I.D., T. Tsujimoto, M. Barnes-Davies, M.F. Cuttle, and T. Takahashi. 1998. Inactivation of presynaptic calcium current contributes to synaptic depression at a fast central synapse. *Neuron*. 20:797–807. [https://doi.org/10.1016/S0896-6273\(00\)81017-X](https://doi.org/10.1016/S0896-6273(00)81017-X)
- Hatakeyama, S., M. Wakamori, M. Ino, N. Miyamoto, E. Takahashi, T. Yoshinaga, K. Sawada, K. Imoto, I. Tanaka, T. Yoshizawa, et al. 2001. Differential nociceptive responses in mice lacking the α_{1B} subunit of N-type Ca²⁺ channels. *Neuroreport*. 12:2423–2427. <https://doi.org/10.1097/00001756-200108080-00027>
- Hille, B. 1994. Modulation of ion-channel function by G-protein-coupled receptors. *Trends Neurosci.* 17:531–536. [https://doi.org/10.1016/0166-2236\(94\)90157-0](https://doi.org/10.1016/0166-2236(94)90157-0)
- Hirning, L.D., A.P. Fox, E.W. McCleskey, B.M. Olivera, S.A. Thayer, R.J. Miller, and R.W. Tsien. 1988. Dominant role of N-type Ca²⁺ channels in evoked release of norepinephrine from sympathetic neurons. *Science*. 239:57–61. <https://doi.org/10.1126/science.2447647>
- Holz, G.G. IV, K. Dunlap, and R.M. Kream. 1988. Characterization of the electrically evoked release of substance P from dorsal root ganglion neurons: methods and dihydropyridine sensitivity. *J. Neurosci.* 8:463–471.
- Inchauspe, C.G., F.J. Martini, I.D. Forsythe, and O.D. Uchitel. 2004. Functional compensation of P/Q by N-type channels blocks short-term plasticity at the calyx of Held presynaptic terminal. *J. Neurosci.* 24:10379–10383. <https://doi.org/10.1523/JNEUROSCI.2104-04.2004>
- Jun, K., E.S. Piedras-Rentería, S.M. Smith, D.B. Wheeler, S.B. Lee, T.G. Lee, H. Chin, M.E. Adams, R.H. Scheller, R.W. Tsien, and H.S. Shin. 1999. Ablation of P/Q-type Ca²⁺ channel currents, altered synaptic transmission, and progressive ataxia in mice lacking the

- α_{1A} -subunit. *Proc. Natl. Acad. Sci. USA*. 96:15245–15250. <https://doi.org/10.1073/pnas.96.26.15245>
- Kawasaki, H., and R.H. Kretsinger. 1995. Calcium-binding proteins I: EF-hands. *Protein Profile*. 2:297–490.
- Kim, E.Y., C.H. Rumpf, Y. Fujiwara, E.S. Cooley, F. Van Petegem, and D.L. Minor Jr. 2008. Structures of Ca_v2 Ca^{2+} /CaM-IQ domain complexes reveal binding modes that underlie calcium-dependent inactivation and facilitation. *Structure*. 16:1455–1467. <https://doi.org/10.1016/j.str.2008.07.010>
- Kim, E.Y., C.H. Rumpf, F. Van Petegem, R.J. Arant, F. Findeisen, E.S. Cooley, E.Y. Isacoff, and D.L. Minor Jr. 2010. Multiple C-terminal tail Ca^{2+} /CaMs regulate $\text{Ca}_v1.2$ function but do not mediate channel dimerization. *EMBO J*. 29:3924–3938. <https://doi.org/10.1038/emboj.2010.260>
- Kim, J., S. Ghosh, D.A. Nunziato, and G.S. Pitt. 2004. Identification of the components controlling inactivation of voltage-gated Ca^{2+} channels. *Neuron*. 41:745–754. [https://doi.org/10.1016/S0896-6273\(04\)00081-9](https://doi.org/10.1016/S0896-6273(04)00081-9)
- Lee, A., S.T. Wong, D. Gallagher, B. Li, D.R. Storm, T. Scheuer, and W.A. Catterall. 1999. Ca^{2+} /calmodulin binds to and modulates P/Q-type calcium channels. *Nature*. 399:155–159. <https://doi.org/10.1038/20194>
- Lee, A., T. Scheuer, and W.A. Catterall. 2000. Ca^{2+} /calmodulin-dependent facilitation and inactivation of P/Q-type Ca^{2+} channels. *J. Neurosci*. 20:6830–6838.
- Lee, A., H. Zhou, T. Scheuer, and W.A. Catterall. 2003. Molecular determinants of Ca^{2+} /calmodulin-dependent regulation of $\text{Ca}_v2.1$ channels. *Proc. Natl. Acad. Sci. USA*. 100:16059–16064. <https://doi.org/10.1073/pnas.2237000100>
- Li, B., H. Zhong, T. Scheuer, and W.A. Catterall. 2004. Functional role of a C-terminal Gbetagamma-binding domain of $\text{Ca}_v2.2$ channels. *Mol. Pharmacol*. 66:761–769.
- Liang, H., C.D. DeMaria, M.G. Erickson, M.X. Mori, B.A. Alseikhan, and D.T. Yue. 2003. Unified mechanisms of Ca^{2+} regulation across the Ca^{2+} channel family. *Neuron*. 39:951–960. [https://doi.org/10.1016/S0896-6273\(03\)00560-9](https://doi.org/10.1016/S0896-6273(03)00560-9)
- Lipscombe, D., S.E. Allen, and C.P. Toro. 2013. Control of neuronal voltage-gated calcium ion channels from RNA to protein. *Trends Neurosci*. 36:598–609. <https://doi.org/10.1016/j.tins.2013.06.008>
- Maggi, C.A., M. Tramontana, R. Cecconi, and P. Santicoli. 1990. Neurochemical evidence for the involvement of N-type calcium channels in transmitter secretion from peripheral endings of sensory nerves in guinea pigs. *Neurosci. Lett*. 114:203–206. [https://doi.org/10.1016/0304-3940\(90\)90072-H](https://doi.org/10.1016/0304-3940(90)90072-H)
- Maximov, A., and I. Bezprozvanny. 2002. Synaptic targeting of N-type calcium channels in hippocampal neurons. *J. Neurosci*. 22:6939–6952.
- Mintz, I.M., B.L. Sabatini, and W.G. Regehr. 1995. Calcium control of transmitter release at a cerebellar synapse. *Neuron*. 15:675–688. [https://doi.org/10.1016/0896-6273\(95\)90155-8](https://doi.org/10.1016/0896-6273(95)90155-8)
- Mori, M.X., C.W. Vander Kooi, D.J. Leahy, and D.T. Yue. 2008. Crystal structure of the Ca_v2 IQ domain in complex with Ca^{2+} /calmodulin: high-resolution mechanistic implications for channel regulation by Ca^{2+} . *Structure*. 16:607–620. <https://doi.org/10.1016/j.str.2008.01.011>
- Nanou, E., J. Yan, N.P. Whitehead, M.J. Kim, S.C. Froehner, T. Scheuer, and W.A. Catterall. 2016. Altered short-term synaptic plasticity and reduced muscle strength in mice with impaired regulation of presynaptic $\text{Ca}_v2.1$ Ca^{2+} channels. *Proc. Natl. Acad. Sci. USA*. 113:1068–1073. <https://doi.org/10.1073/pnas.1524650113>
- Patil, P.G., D.L. Brody, and D.T. Yue. 1998. Preferential closed-state inactivation of neuronal calcium channels. *Neuron*. 20:1027–1038. [https://doi.org/10.1016/S0896-6273\(00\)80483-3](https://doi.org/10.1016/S0896-6273(00)80483-3)
- Pedigo, S., and M.A. Shea. 1995. Quantitative endoprotease GluC footprinting of cooperative Ca^{2+} binding to calmodulin: Proteolytic susceptibility of E31 and E87 indicates interdomain interactions. *Biochemistry*. 34:1179–1196. <https://doi.org/10.1021/bi00004a011>
- Peterson, B.Z., C.D. DeMaria, J.P. Adelman, and D.T. Yue. 1999. Calmodulin is the Ca^{2+} sensor for Ca^{2+} -dependent inactivation of L-type calcium channels. *Neuron*. 22:549–558. [https://doi.org/10.1016/S0896-6273\(00\)80709-6](https://doi.org/10.1016/S0896-6273(00)80709-6)
- Peterson, B.Z., J.S. Lee, J.G. Mülle, Y. Wang, M. de Leon, and D.T. Yue. 2000. Critical determinants of Ca^{2+} -dependent inactivation within an EF-hand motif of L-type Ca^{2+} channels. *Biophys. J*. 78:1906–1920. [https://doi.org/10.1016/S0006-3495\(00\)76739-7](https://doi.org/10.1016/S0006-3495(00)76739-7)
- Pitt, G.S., R.D. Zühlke, A. Hudmon, H. Schulman, H. Reuter, and R.W. Tsien. 2001. Molecular basis of calmodulin tethering and Ca^{2+} -dependent inactivation of L-type Ca^{2+} channels. *J. Biol. Chem*. 276:30794–30802. <https://doi.org/10.1074/jbc.M104959200>
- Sakaba, T., and E. Neher. 2001. Quantitative relationship between transmitter release and calcium current at the calyx of held synapse. *J. Neurosci*. 21:462–476.
- Sang, L., I.E. Dick, and D.T. Yue. 2016. Protein kinase A modulation of $\text{Ca}_v1.4$ calcium channels. *Nat. Commun*. 7:12239. <https://doi.org/10.1038/ncomms12239>
- Simms, B.A., and G.W. Zamponi. 2014. Neuronal voltage-gated calcium channels: structure, function, and dysfunction. *Neuron*. 82:24–45. <https://doi.org/10.1016/j.neuron.2014.03.016>
- Tang, Q., M.L. Bangaru, S. Kostic, B. Pan, H.E. Wu, A.S. Koopmeiners, H. Yu, G.J. Fischer, J.B. McCallum, W.M. Kwok, et al. 2012. Ca^{2+} -dependent regulation of Ca^{2+} currents in rat primary afferent neurons: Role of CaMKII and the effect of injury. *J. Neurosci*. 32:11737–11749. <https://doi.org/10.1523/JNEUROSCI.0983-12.2012>
- Theoharis, N.T., B.R. Sorensen, J. Theisen-Toupal, and M.A. Shea. 2008. The neuronal voltage-dependent sodium channel type IIQ motif lowers the calcium affinity of the C-domain of calmodulin. *Biochemistry*. 47:112–123. <https://doi.org/10.1021/bi7013129>
- Thomas, J.R., and A. Lee. 2016. Measuring Ca^{2+} -dependent modulation of voltage-gated Ca^{2+} channels in HEK-293T cells. *Cold Spring Harb. Protoc*. 2016:pdb.prot087213. <https://doi.org/10.1101/pdb.prot087213>
- Tsujimoto, T., A. Jeromin, N. Saitoh, J.C. Roder, and T. Takahashi. 2002. Neuronal calcium sensor 1 and activity-dependent facilitation of P/Q-type calcium currents at presynaptic nerve terminals. *Science*. 295:2276–2279. <https://doi.org/10.1126/science.1068278>
- Wheeler, D.B., A. Randall, and R.W. Tsien. 1994. Roles of N-type and Q-type Ca^{2+} channels in supporting hippocampal synaptic transmission. *Science*. 264:107–111. <https://doi.org/10.1126/science.7832825>
- Wu, J., Z. Yan, Z. Li, X. Qian, S. Lu, M. Dong, Q. Zhou, and N. Yan. 2016. Structure of the voltage-gated calcium channel $\text{Ca}_v1.1$ at 3.6 Å resolution. *Nature*. 537:191–196. <https://doi.org/10.1038/nature19321>